Modelling the Solubility of H_2S and CO_2 in Ionic Liquids Using PC-SAFT Equation of State

Heba Al-fnaish[1,*], Leo Lue[1]

Department of Chemical and Process Engineering, University of Strathclyde, 75 Montrose Street, Glasgow G1 1XJ, United Kingdom

Abstract

The Perturbed Chain Statistical Association Fluid Theory (PC-SAFT) is used to investigate the solubility of carbon dioxide (CO_2) and hydrogen sulfide (H_2S) in several methylimidazolium bis (trifluoromethylsulfonyl) imide ionic liquids (ILs) or [$C_n$mim][NTf_2] where n = 2, 4, 6, and 8. The pure component parameters of the ILs are estimated by fitting to experimental density data and binary solubility data of acid gases in ILs reported in literature. Two strategies are examined to model the ILs. In the first strategy, the ILs are treated as neutral molecules. In the second strategy, the ILs are modelled as two charged ions: imidazolium cation $[C_n\text{mim}]^+$ and bis (trifluoromethylsulfonyl) imide anion $[NTf_2]^-$. For each strategy, four different self association schemes are examined: non-associating, 2-site, 3-site, and 4-site schemes. The inclusion of self-association of the IL improves the calculated acid gas solubility. The 4-site association scheme with two donors and two acceptors provided the best results for almost all the investigated acid gases-IL binary systems, with an AARD of 2.76%–6.62% for H_2S-ILs systems and 1.54%–4.98% for CO_2-IL systems. Using these parameters, the solubility of ternary systems of CO_2 and H_2S in C_8mimNTf_2 IL is successfully represented, with an AARD of 6.24% for CO_2 and 7.99% for H_2S, without the need for binary interaction parameters. The high pressure density of ILs and the binary solubility of CO_2-ILs at high pressure is also represented with reasonable accuracy. The inclusion of the electrolyte term in the second strategy improves the high pressure density and solubility results as well as the predictive capability of the model by allowing for the examination of the effect of using different cation-anion combinations.

Keywords: Solubility, acid gases, ionic liquids, PC-SAFT

1. Introduction

Due to its lower carbon content compared to oil and coal, natural gas is considered the most environmentally benign fossil fuel. However, raw gas still needs to be treated to remove acid gases such as carbon dioxide (CO_2) and hydrogen sulfide (H_2S) mainly because of their corrosive nature, toxicity and flammability. CO_2 may also freeze, causing blockage of pipelines [1], and has a poor heating value, which lowers the heating value of the gas [2]. Numerous technologies are available for acid gas removal from natural gas. Alkanolamine based chemical absorption is the most commercially utilized process, due to its versatility, efficiency, and low solvent cost. However, alkanolamines are volatile, corrosive, and their regeneration process is highly energy intensive, comprising 70% of the total operating costs [3, 4].

Recently, ionic liquids (ILs) have emerged as an alternative physical solvent for alkanolamines. ILs are organic salts characterized by their negligible volatility, high thermal stability, high ionic conductivity, and structural tunability. They are liquids over a wide range of temperatures; they can have melting points ranging from −100–200°C [3], which is much lower than the melting points of conventional ionic compounds, such as sodium chloride.

An IL consists of two types of ions: an organic cation, such as imidazolium, pyridinium or phosphonium ions and an inorganic anion, such as Cl^-, BF_4^-, PF_6^-, $CF_3SO_3^-$, NTf_2^-, or an organic anion such as carboxylate (RCO_2^-) [5]. ILs can be used in a variety of applications, including catalysis, gas storage and separation [6]. By replacing volatile and possibly toxic organic solvents, ILs have the potential to contribute significantly to im-

*Corresponding author

Email addresses: heba.al-fnaish@strath.ac.uk (Heba Al-fnaish), leo.lue@strath.ac.uk (Leo Lue)

proving the safety, economy and environmental sustainability of acid gas removal processes [7]. Due to their negligible volatility and high thermal stability, the use of ILs for sweetening can reduce the solvent losses, thermal decomposition and the consequent environmental impact. According to Kumar et al. [3], using ILs for the gas sweetening can lead to an overall reduction in energy consumption because physical absorption takes place, rather than chemical absorption.

Over the past few years, a significant number of experimental and theoretical studies of ILs and their mixtures with gas species has been published. Most of the experimental studies reported in literature focused on CO_2 capture, and less attention has been paid to H_2S removal. Many studies provided experimental measurements for the solubility of CO_2 in different types of ILs. The investigated ILs were either conventional ILs [8, 9, 10], task specific (TSILs) for CO_2 capture [11], or functionalized ILs [12] with amine or hydroxyl group attached to the cation of the IL. Generally, all types of ILs showed either comparable or superior CO_2 uptake to traditional alkanolamine solvents. However, both functionalized and TSILs are highly viscous, and their production requires several synthetic and purification stages [11]. Camper et al. [13] presented an attractive method using amine-IL solutions as an alternative to the viscous and complex functionalized ILs and TSILs. Some research studies provided measurements for H_2S solubility in different ILs with comparison to CO_2 and other gases [14, 15, 16, 17]. In all the studies, H_2S showed higher solubilities than CO_2 and other gases in the ILs. Pomelli et al. [15] attributed that to the presence of specific interactions between H_2S and the ILs and used quantum chemical calculations to investigate the influence of these interactions on the H_2S solubility at the molecular level.

The high solubility of H_2S and CO_2 in different ILs, compared to that in conventional alkanolamine suggests that ILs can be more efficiently used as solvents for acid gas separation from natural gas. Furthermore, as H_2S is more soluble than CO_2 in ILs, ILs can be utilized for the separation of the two gases from each other.

Theoretically, both molecular simulation and thermodynamic modelling have been used to describe the molecular structure, phase behavior and thermodynamic properties of a certain system. Molecular simulations have been used by many authors to study the microscopic structure of ILs and their properties [18, 19, 20, 21, 22, 23, 24, 25, 26]. They provide a tool for screening different ILs before using them for certain applications [27]. However, due to their computational expense, these methods have limited use in process simulation.

An alternative approach for describing the behavior of ILs and their mixtures theoretically is the thermodynamic modelling. Thermodynamic models used for this purpose have been classified by Vega et al. [27] into four categories: cubic equations, activity coefficient methods, quantum mechanics-based methods, and statistical mechanics-based molecular approaches.

Shariati and Peters [28] and Shiflett and Yokozeki [29] used the Peng-Robinson [30] and Redlich-Kwong [31] equations of state, respectively, to model the phase behavior and the solubility of the binary and ternary systems of acid gases in ILs. The systems were successfully described at low to moderate pressures; however, the agreement was poor at high pressure. Two activity coefficient models have been used for the thermodynamic modelling of IL containing systems are the Non-Random Two-Liquid model [32] and the UNIversal QUAsi Chemical model [33]. Both models were successfully used to describe the LLE and SLE data of different binary and ternary IL containing systems with superior results for the UNIQUAC model over the NRTL model [34, 35].

Group contribution methods, such as UNIFAC [36] and modified UNIFAC [37], have also been used to estimate several IL properties such as density, surface tension, viscosity, speed of sound, liquid heat capacity and transport properties [38, 39, 40, 41, 42]. The phase equilibrium of IL binary and ternary systems containing alkanes, alkenes, aromatics, alcohols, ketones and water have also been investigated using group contribution approach [41, 43, 42].

The conductor-like screening model for real solvents (COSMO-RS) developed by Klamt [44] is another approach used by some authors [45, 46, 47] for the prediction of phase equilibria of IL systems. It employs the results obtained from quantum chemistry calculations to calculate the activity coefficients and, hence, predict the phase equilibria.

Recently, statistical mechanics-based free energy models have gained a considerable attention in modelling IL systems. These models account explicitly for the microscopic characteristics of IL mixtures. The original Statistical Associating Fluid Theory (SAFT) proposed by Chapman et al. [48] and Huang and Radosz [49] has been modified by many authors to produce different versions of the models for different systems. Some common versions include SAFT-VR for chain molecules of variable range potential [50], soft-SAFT for complex fluid mixtures [51], the group contribution SAFT-γ [52], and PC-PolarSAFT and truncated PC-PolarSAFT [53] for polar and associating fluid sys-

tems.

All of these models have been successfully used to represent the solubility of H_2S, CO_2, and other gases in some ILs and to measure the thermodynamic properties of the IL-containing mixture [54, 55, 56, 57]. However, in most cases, binary interactions parameters, found by fitting to experimental data, have been used to enhance the accuracy of the VLE results; these parameters may be dependent or independent of temperature.

The aim of this work is to examine the ability of the PC-SAFT model developed by Gross and Sadowski [58] to represent the solubility of CO_2 and H_2S in several methylimidazolium bis (trifluoromethylsulfonyl) imide ILs without the need for binary interaction parameters. It is generally accepted that ILs cations and anions associate forming hydrogen bonds [59]. The typical hydrogen bond is defined as a bond formed between two molecules, one containing an electro-negative atom (possessing lone pairs of electrons) such as O, N, or F referred to as proton acceptor and another containing a covalent bond between hydrogen and an electronegative atom such as O, N or S referred to as proton donor [60]. However, covalent bonds with less electronegative atoms such as C, Se and Si, are now recognized as proton donors [59]. For the studied ILs, we consider the hydrogen bonds formed between any of the covalent C-H bonds on the methylimidazolium cation ring (proton donors, circled in red in Figure 1) and any of the four oxygen atoms on bis (trifluoromethylsulfonyl) imide anion (proton acceptors, circled in blue in Figure 1). The hydrogen bonding here could takes place between two IL molecules or between the cation and the anion of the same IL molecule. The effect of accounting for the IL cation-anion association interaction with different association schemes is examined here. To the best of our knowledge, the effect of changing the association scheme has not been examined yet.

Two strategies are adopted in this work to model the ILs. In the first strategy, ILs are modelled as neutral molecules and only the hard chain, the dispersion and the association contribution to Helmholtz free energy are considered. In the second strategy, ILs are modelled as two-part charged ions and the electrolyte contribution to Helmholtz free energy is also considered to account for the electrostatic attraction between charged ions. The purpose of applying this strategy is to enhance the predictive capability of the model by allowing us to try different IL cation-anion combinations in the future. For the first time, four different association schemes for ILs are examined for both strategies: non-associating scheme, 2-sites scheme (one donor and one acceptor), 3-sites scheme (two donors and one acceptor) and 4-sites scheme (two donors and two acceptors). Our interest is mainly focused on finding the best strategy and association scheme to represent the solubility of acid gases in ILs without the need for any binary interaction parameters to be used in modelling the acid gas removal problem that utilizes ILs as an alternative to alkanolamines.

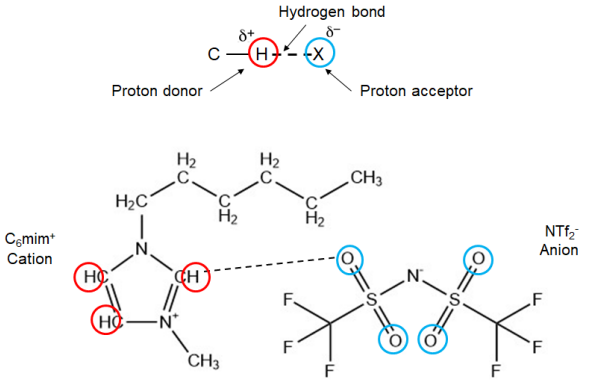

Figure 1: Illustrative example of hydrogen bonding between $[C_6mim]^+$ cation and $[NTf_2]^-$ anion in 1-hexyl-3-methylimidazolium bis(trifluoromethanesulfonyl)amide IL: Strategy 2, 2-site scheme (one donor and one acceptor).

The remainder of this paper is organized as follows. The following section defines the PC-SAFT model and the different Helmhotz free energy contributions considered in this study. The pure component parameters for the acid gases and the studied ILs are presented and discussed in Section 3. The solubility calculations and results are presented and analyzed in Section 4 for binary mixtures and in Section 5 for ternary mixtures. Finally, the main findings are summarized in Section 6.

2. Theory

The PC-SAFT EOS originally developed by Gross and Sadowski [58] was used in this study to represent the solubility of acid gases in several methylimidazolium bis (trifluoromethylsulfonyl) imide ILs. PC-SAFT represents the molecule as a chain of m_i spherical segments of diameter σ_i, as illustrated in Figure 2. For non-associating, neutral molecules, the molecules interact only through excluded volume and dispersion forces; therefore in this case, three molecular parameters are required to describe the molecules: m_i, σ_i, and the strength ε_i of the dispersion interaction.

For associating molecules (e.g., molecules that tend to form hydrogen bonds), two more additional parameters are required: the association energy $\varepsilon^{A_iB_i}$ between

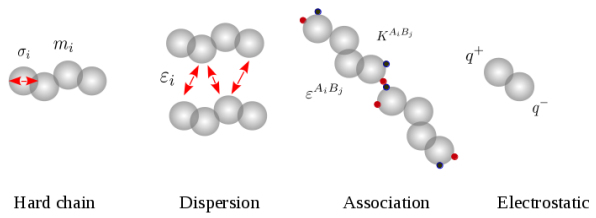

Figure 2: Illustration of PC-SAFT molecular parameters and the contributions to the Helmholtz free energy.

sites A and B on molecule i and the effective association volume $K^{A_iB_i}$ between site A and B on the same molecule. For charged ions or electrolytes, the Debye-Hückel term [61] is added to account for the long range Coulomb forces among ions in the system. In this case, the charge q_i of each ion is required.

Within PC-SAFT, the Helmholtz free energy is expressed as a sum of separate contributions from different physical effects.

The residual Helmholtz free energy per molecules is given by

$$a^{res} = a^{hc} + a^{disp} + a^{assoc} + a^{elec}, \tag{1}$$

where a^{hc} is the hard-chain reference contribution, $a^{disp}$is the dispersion contribution, a^{assoc} is the association contribution, and a^{elec} is the electrolyte contribution. The expressions for each of these terms will be summarized below, however, the reader is referred to Refs. 58, 48, and 62 for more detailed discussions of different contributions to Helmholtz free energy.

The hard-chain reference contribution is given by

$$a^{\mathrm{hc}} = ma^{\mathrm{hs}} - k_BT\sum_i x_i(m_i - 1)\ln g_{ii}^{hs} \tag{2}$$

where k_B is the Boltzmann constant, T is the absolute temperature of the system, x_i is the mole fraction of molecules of type i in the system, and $m = \sum_i x_i m_i$. The quantity g_{ii}^{hs} is the contact value of the radial distribution function, given as:

$$\begin{aligned} g_{ij}^{hs} = &\frac{1}{(1-\zeta_3)} + \left(\frac{d_i d_j}{d_i + d_j}\right)\frac{3\zeta_2}{(1-\zeta_3)^2} \\ &+ \left(\frac{d_i d_j}{d_i + d_j}\right)^2 \frac{2\zeta_2^2}{(1-\zeta_3)^3}. \end{aligned} \tag{3}$$

where d_i is a temperature-dependent segment diameter of component i and defined as:

$$d_i = \sigma_i\left[1 - 0.12\exp\left(-\frac{3\varepsilon_i}{k_BT}\right)\right], \tag{4}$$

ζ_n is given as:

$$\zeta_n = \frac{\pi}{6}\rho\sum_i x_i m_i d_i^n, \tag{5}$$

and ρ is the number density of molecules in the system.

The hard-sphere contribution to Helmholtz free energy is:

$$a^{hs} = \frac{k_BT}{\zeta_0}\left[\frac{3\zeta_1\zeta_2}{(1-\zeta_3)} + \frac{\zeta_2^3}{\zeta_3(1-\zeta_3)^2} + \left(\frac{\zeta_2^3}{\zeta_3^2} - \zeta_0\right)\ln(1-\zeta_3)\right] \tag{6}$$

The dispersion contribution to the Helmholtz free energy is given by:

$$\begin{aligned} \frac{a^{disp}}{k_BT} = &-2\pi\rho I_1(\zeta_3, m)\overline{m^2\varepsilon\sigma^3} \\ &- \pi\rho m C_1 I_2(\zeta_3, m)\overline{m^2\varepsilon^2\sigma^3} \end{aligned} \tag{7}$$

with

$$\begin{aligned} C_1 &= \left(1 + Z^{hc} + \rho\frac{\partial Z^{hc}}{\partial\rho}\right)^{-1} \\ &= \left(1 + m\frac{8\zeta_3 - 2\zeta_3^2}{(1-\zeta_3)^4} + (1-m)\frac{20\zeta_3 - 27\zeta_3^2 + 12\zeta_3^3 - 2\zeta_3^4}{[(1-\zeta_3)(2-\zeta_3)]^2}\right) \end{aligned} \tag{8}$$

and

$$\overline{m^2\varepsilon\sigma^3} = \sum_{ij} x_i x_j m_i m_j\left(\frac{\varepsilon_{ij}}{k_BT}\right)\sigma_{ij}^3 \tag{9}$$

$$\overline{m^2\varepsilon^2\sigma^3} = \sum_{ij} x_i x_j m_i m_j\left(\frac{\varepsilon_{ij}}{k_BT}\right)^2\sigma_{ij}^3 \tag{10}$$

The Lorentz-Berthelot mixing rules were employed to determine the parameters σ_{ij} and ε_{ij} between unlike segments:

$$\sigma_{ij} = \frac{1}{2}(\sigma_i + \sigma_j) \tag{11}$$

$$\varepsilon_{ij} = \sqrt{\varepsilon_i\varepsilon_j}(1 - k_{ij}) \tag{12}$$

The quantities $I_1(\zeta_3, m)$ and $I_2(\zeta_3, m)$ in Eq. (7) above are the integrals of the perturbation theory and are expressed as a power series in density as below

$$I_1(\zeta_3, m) = \sum_{i=0}^{6} a_i(m)\zeta_3^i \tag{13}$$

$$I_2(\zeta_3, m) = \sum_{i=0}^{6} b_i(m)\zeta_3^i \tag{14}$$

The coefficients of the power series are related to the segment number m as follows

$$a_i(m) = a_{0i} + \frac{m-1}{m}a_{1i} + \frac{m-1}{m}\frac{m-2}{m}a_{2i} \quad (15)$$

$$b_i(m) = b_{0i} + \frac{m-1}{m}b_{1i} + \frac{m-1}{m}\frac{m-2}{m}b_{2i} \quad (16)$$

where a_{0i}, a_{1i}, a_{2i}, b_{0i}, b_{1i}, and b_{2i} are the universal PC-SAFT constants, which can be found in Ref. 58.

The association contribution to Helmholtz free energy is given by [48]

$$\frac{a^{\text{assoc}}}{k_BT} = \sum_i^c x_i \left[\sum_{A_i}\left(\ln X^{A_i} - \frac{X^{A_i}}{2}\right) + \frac{1}{2}M_i\right] \quad (17)$$

where X^{A_i} is the mole fraction of molecule i not bonded at site A, and M_i is the total number of association sites (both donor and acceptor sites) on molecule i. The quantities X^{A_i} can be determined by solving the equations:

$$X^{A_i} = \left[1 + N_{Av}\rho \sum_{j,B_j} x_j X^{B_j}\Delta^{A_iB_j}\right]^{-1} \quad (18)$$

where the index B_j runs over all association sites on molecule j, and $\Delta^{A_iB_j}$ is the association strength and is defined as

$$\Delta^{A_iB_j} = g_{ij}^{hs}\left[e^{\varepsilon^{A_iB_j}/(k_BT)} - 1\right]\sigma_{ij}^3 K^{A_iB_j} \quad (19)$$

where $\varepsilon^{A_iB_j}$ is the association energy, and $K^{A_iB_j}$ is the effective association volume between a site A on molecule i and a site B on molecule j

For systems with charged components, the electrolyte term a^{elec}, as given by the Debye-Hückel theory [61], is added to contributions of Helmholtz free energy. Within the Debye-Hückel theory of electrolyte solutions, the ions are treated as spheres with charge q_i that can approach each other to within an effective ion diameter a_i and that are immersed in a background solvent characterized by a dielectric constant ϵ.

The resulting expression for the molar Helmholtz free energy is

$$a^{elec} = -\frac{\kappa}{12\pi\epsilon}\sum_i x_i q_i^2 \chi_i \quad (20)$$

where the quantity χ_i is defined as

$$\chi_i = \frac{3}{(\kappa a_i)^3}\left[\frac{3}{2} + \ln(1+\kappa a_i) - 2(1+\kappa a_i) + \frac{1}{2}(1+\kappa a_i)^2\right], \quad (21)$$

Table 1: PC-SAFT pure component parameters for acid gases used in this study.

Component	MW	T range	m_i	σ_i	ε_i/k_B	P^{sat}	ρ^{sat}	Ref.
	g mol^{-1}	K		Å	K	AARD %	AARD %	
CO_2	44.01	216–304	2.0729	2.7852	169.21	3.25	1.93	[58]
H_2S	34.08	187–362	1.6686	3.0349	229.00	0.40	0.80	[65]

where κ is the inverse Debye screening length defined by [62] as

$$\kappa = \sqrt{\frac{4\pi\rho}{\epsilon k_BT}\sum_j q_j^2 x_j} \quad (22)$$

In this work, both acid gases are treated as non associating and non electrolyte components and cross association between acid gases and ILs is not considered. For the ionic liquid molecules two strategies are adopted. In the first strategy, ILs are modelled as neutral molecules and only the hard chain, the dispersion and the association contribution to Helmholtz free energy are considered. In the second strategy, the ionic liquids are modelled [63] as fully dissociated ions (cations and anions). The charge of each ion is assumed to be localized within a segment, and, consequently, we choose $a_i = \sigma_i$. The dielectric constant of the medium ϵ is set to unity in all cases, following Ji et al. [64].

Association within the ionic liquids is also considered in this work. In strategy 1, the association takes place between the neutral IL molecules where the proton donor is from one molecule and the acceptor from another molecule. In strategy 2, the association takes place between the cation and the anion of the same IL as illustrated in Figure 1.

3. PC-SAFT Pure Component Parameters

3.1. Acid Gases

Both acid gases, CO_2 and H_2S, are treated as non associating components, and the cross-association between the acid gases and the ILs is not considered in this work. Only three molecular parameters are required to describe each component within the PC-SAFT model: the number of segments m_i, the segment diameter σ_i, and the depth of square well interaction potential ε_i. The parameters values for the acid gases are taken from Refs. 58 and 65 and are reported in Table 1.

In order to validate these parameters, we used them to represent the vapor pressure for both acid gases using PC-SAFT. The calculations were able to successfully reproduce the experimentally measured vapor pressure data from [66] with reasonable accuracy (3.25% AARD

for CO_2 and 0.4% for H_2S). The vapor pressure curves are shown in Figure 3. The saturated liquid density of both gases is also calculated using the PC-SAFT parameters in Table 1 and compared to the experimental measurements from [66]. The density was satisfactorily represented with AARD of 1.93% for CO_2 and 0.8% for H_2S. At 298 K, the saturated liquid density of CO_2 calculated using PC-SAFT was 724.5 kg m^{-3} and that of H_2S was 783.8 kg m^{-3}.

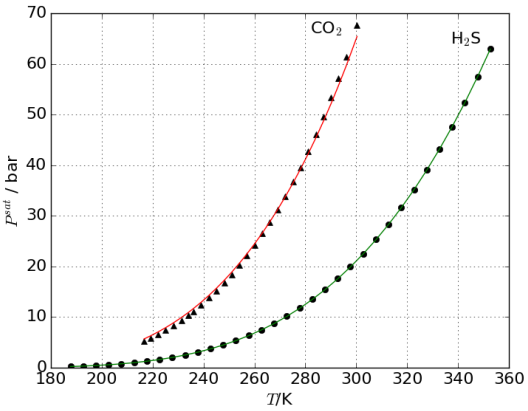

Figure 3: Vapor pressure of acid gases CO_2 (red lines and triangles) and H_2S (green lines and triangles). The symbols represent the experimental vapor pressure data taken from Ref. 66. The lines are the vapor pressures calculated using PC-SAFT with the parameters given in Table 1.

3.2. Ionic Liquids

Four methylimidazolium bis (trifluoromethylsulfonyl) imide or [$C_n$mim][NTf_2] ILs with n = 2, 4, 6, and 8 are investigated in this work. The ILs are modelled using the two strategies described in the previous section.

The proton donor could be one of the three hydrogen atoms covalently bonded to the carbons on the imidazolium ring. The proton acceptor could be any of the four oxygen atoms on the [NTf_2] anion. The possible donor and acceptor sites are highlighted in Figure 1. In this work, four association schemes are investigated: a non-associating scheme (where association is neglected), a 2-site scheme (one donor and one acceptor), a 3-site scheme (two donors and one acceptor), and a 4-site scheme (two donors and two acceptors).

Without association, only three molecular parameters are required to describe each IL using PC-SAFT: m, σ and ε. When self-association is included, two additional parameters are needed for each IL: the association energy $\varepsilon^{A_iB_i}$ between donor site A and acceptor site B on the molecule and the effective association volume $K^{A_iB_i}$ between sites A and B.

The values of the pure component parameters m_i, σ_i, ε_i, $\varepsilon^{A_iB_i}$ and $K^{A_iB_i}$ for the four studied ILs are determined by fitting to experimental density data recorded in literature at atmospheric pressure [67, 68, 69]. This is performed by using the Levenberg-Marquardt algorithm within the LMFIT [70] software package to minimize the objective function OF:

$$OF = \sum_{i=1}^{n} \left(\rho_i^{exp} - \rho_i^{cal}\right)^2 \tag{23}$$

where n is the number of data points, ρ_i^{exp} is the experimental density at a particular temperature and ρ_i^{cal} is the density calculated using PC-SAFT EOS.

The average absolute relative deviation (AARD) between the calculated and the experimental data is calculated as:

$$AARD = \frac{1}{n} \sum_{i=1}^{n} \left| \frac{\rho_i^{exp} - \rho_i^{cal}}{\rho_i^{exp}} \right|. \tag{24}$$

The AARD of the calculated density at low pressure is in the range of 0.07%–0.38%. The results of the 4-site scheme for fitting the density of all ILs using strategy 1 are shown in Figure 4. There was no significant difference in the calculated density between the different association schemes and between the two strategies at low pressure; therefore, only the results of the 4-site scheme of strategy 1 are shown in the figure. For C_6mimNTf_2 and C_8mimNTf_2 ILs, the experimental density data available in literature were limited to a narrow temperature range; therefore, their density is extrapolated using PC-SAFT EOS.

The densities of C_2mimNTf_2 and C_4mimNTf_2 at high pressures are shown in Figures 5 and 6, respectively. At these pressures, strategy 2 provides a slightly better fit to the experimental density of the ILs; the AARD of [C_2mim][NTf_2] density at 500 bar is 0.48% for strategy 1 and 0.45% for strategy 2. For [C_4mim][NTf_2], the AARD for the density at 298.15 K and pressures ranging from 0–1500 bar is 0.59% for strategy 1 and 0.27% for strategy 2. Without association, the PC-SAFT predictions for the density of C_2mimNTf_2 at high pressure was better represented using strategy 1 with the AARD ranging from 0.3% at 51 bar to 0.5% at 900 bar. However, strategy 2 performs better when association is included, as compared to the non-associating scheme; the AARD ranges from 0.40% at 51 bar to 0.56% at 900

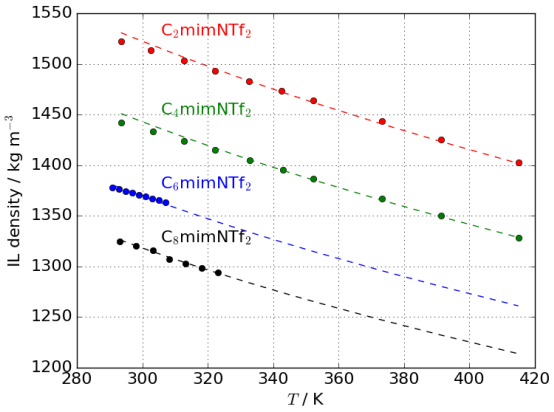

Figure 4: Density variation of the studied ILs with temperature at low pressure: (i) [C_2mim][NTf_2] (red), (ii) [C_4mim][NTf_2] (green), (iii) [C_6mim][NTf_2] (blue), and (iv) [C_8mim][NTf_2] (black). The symbols represent experimental data [67, 68, 69]. The lines are the calculations of PC-SAFT using strategy 1 with the 4-site association scheme.

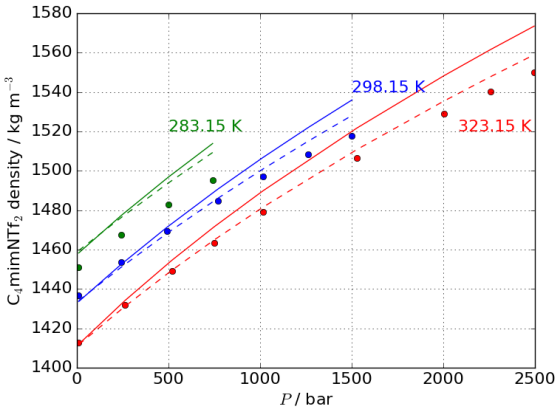

Figure 6: Density of [C_4mim][NTf_2] at high pressure and at different temperatures. The symbols represent experimental data [72]. The dashed lines are the calculations of PC-SAFT using strategy 2 with the 4-site association scheme. The solid lines are calculations using strategy 2 with the non-associating scheme.

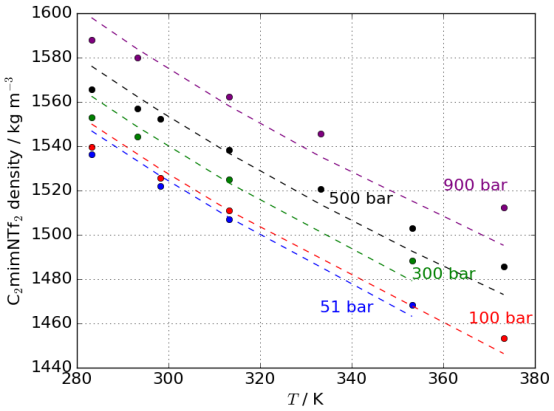

Figure 5: Density of [C_2mim][NTf_2] at high pressures. The symbols represent experimental data [71]. The lines are the calculations of PC-SAFT using strategy 1 with the 4-site association scheme.

bar). For C_4mimNTf_2 at high pressure, including association improves the results for both strategies, with the AARD ranging from 0.2% to 0.9% for pressures up to 2500 bar.

4. Solubility of acid gases in ionic liquids

The PC-SAFT EOS is used to represent the solubility of CO_2 and H_2S in four imidazolium based ILs. As described earlier, two strategies are examined in modelling the ILs; for both strategies, four different association schemes are tested. Phase equilibrium calculations were carried out by equating the fugacities of the acid gas in the vapor and liquid phases. The vapor pressure of the ILs was considered negligible due to their low volatility.

The optimized pure component parameters for PC-SAFT obtained by fitting the experimental density are used to determine the solubility of acid gases in the ILs and adjusted to minimize the AARD of their solubility. The optimum values are those that produce the minimum AARD for both the pure IL density and binary solubility of both acid gases in the IL. Note, however, no cross association between the acid gas and the ILs was included, and no binary interaction parameters were introduced. The optimum PC-SAFT pure component parameters obtained for the studied ILs for the first strategy with different association schemes are reported in Table 2 and in Table 3 for the second strategy.

A summary of the solubility results of both acid gases in the four studied ILs for both strategies with the best association scheme (4-site scheme) and at low pressure (up to 15 bar) is provided in Figure 7. Table 4 summarizes the AARD of all of the investigated systems in this study using both strategies with the 4(2:2) association scheme and the reference of experimental data.

Similar studies were carried out for these same systems by Chen and co-workers [80] and by Li and co-workers [64, 81]. The first strategy is the same as that used by Chen et al. [80] and [64]; however, in their study, only one association scheme was considered for the IL (the 2-site scheme), and despite of using bi-

Table 2: Optimized PC-SAFT Parameters of the studied ILs with Different Association Schemes (ILs as neutral molecules: Strategy 1).

IL	T range K	Association Scheme	σ_i Å	ε_i/k_B K	m_i	$\varepsilon^{A_iB_i}/k_B$ K	$K^{A_iB_i}$	AARD %	ρ_i^{exp} Ref.
$[C_2mim][NTf_2]$	293.49 – 414.92	Non	3.700	380	7.850			0.16	[67]
		2(1:1)	3.580	378	8.694	1350	0.00225	0.18	
		3(2:1)	3.556	378	8.880	1170	0.00225	0.18	
		4(2:2)	3.520	378	9.170	1020	0.00225	0.19	
$[C_4mim][NTf_2]$	293.49 – 414.92	Non	3.780	383	8.360			0.15	[67]
		2(1:1)	3.660	383	9.260	1350	0.00225	0.18	
		3(2:1)	3.640	382	9.410	1170	0.00225	0.18	
		4(2:2)	3.600	382	9.740	1020	0.00225	0.18	
$[C_6mim][NTf_2]$	290.95 – 307.05	Non	3.830	385	9.069			0.08	[68]
		2(1:1)	3.700	383	10.100	1350	0.00225	0.09	
		3(2:1)	3.680	382	10.262	1170	0.00225	0.09	
		4(2:2)	3.635	381	10.660	1020	0.00225	0.09	
$[C_8mim][NTf_2]$	293.15 – 323.15	Non	3.930	387	9.290			0.07	[69]
		2(1:1)	3.790	385	10.400	1350	0.00225	0.07	
		3(2:1)	3.760	384	10.655	1170	0.00225	0.07	
		4(2:2)	3.721	383	11.000	1020	0.00225	0.07	

Table 3: Optimized PC-SAFT Parameters of the studied ILs as dissociated ions with the electrolyte term included (ILs as charged ions: Strategy 2).

IL ion	MW g mol^{-1}	valency	T range K	Association	σ_i Å	ε_i/k_B K	m_i	$\varepsilon^{A_iB_i}/k_B$ K	$K^{A_iB_i}$	AARD %	ρ_i^{exp} Ref.
C_2mim^+	111.168	+1	293.49 – 414.92	Non	3.070	220.00	2.330			0.30	[67]
				2(1:1)	2.900	220.00	2.800	1480	0.00225	0.36	
				3(2:1)	2.795	220.00	3.170	1420	0.00225	0.36	
				4(2:2)	2.664	220.00	3.785	1360	0.00225	0.36	
C_4mim^+	139.221	+1	293.49 – 414.92	Non	3.400	227.00	2.920			0.36	[67]
				2(1:1)	3.220	227.00	3.470	1480	0.00225	0.38	
				3(2:1)	3.120	227.00	3.850	1420	0.00225	0.37	
				4(2:2)	2.970	227.00	4.520	1360	0.00225	0.37	
C_6mim^+	167.215	+1	290.95 – 307.05	Non	3.530	230.00	3.794			0.07	[68]
				2(1:1)	3.325	230.00	4.580	1480	0.00225	0.08	
				3(2:1)	3.230	230.00	5.025	1420	0.00225	0.08	
				4(2:2)	3.080	230.00	5.850	1360	0.00225	0.09	
C_8mim^+	195.335	+1	293.15 – 323.15	Non	3.830	242.00	3.860			0.07	[69]
				2(1:1)	3.620	242.00	4.600	1480	0.00225	0.07	
				3(2:1)	3.500	242.00	5.110	1420	0.00225	0.07	
				4(2:2)	3.340	242.00	5.920	1360	0.00225	0.07	
NTf_2^-	280.145	−1			3.720	375.65	5.960				

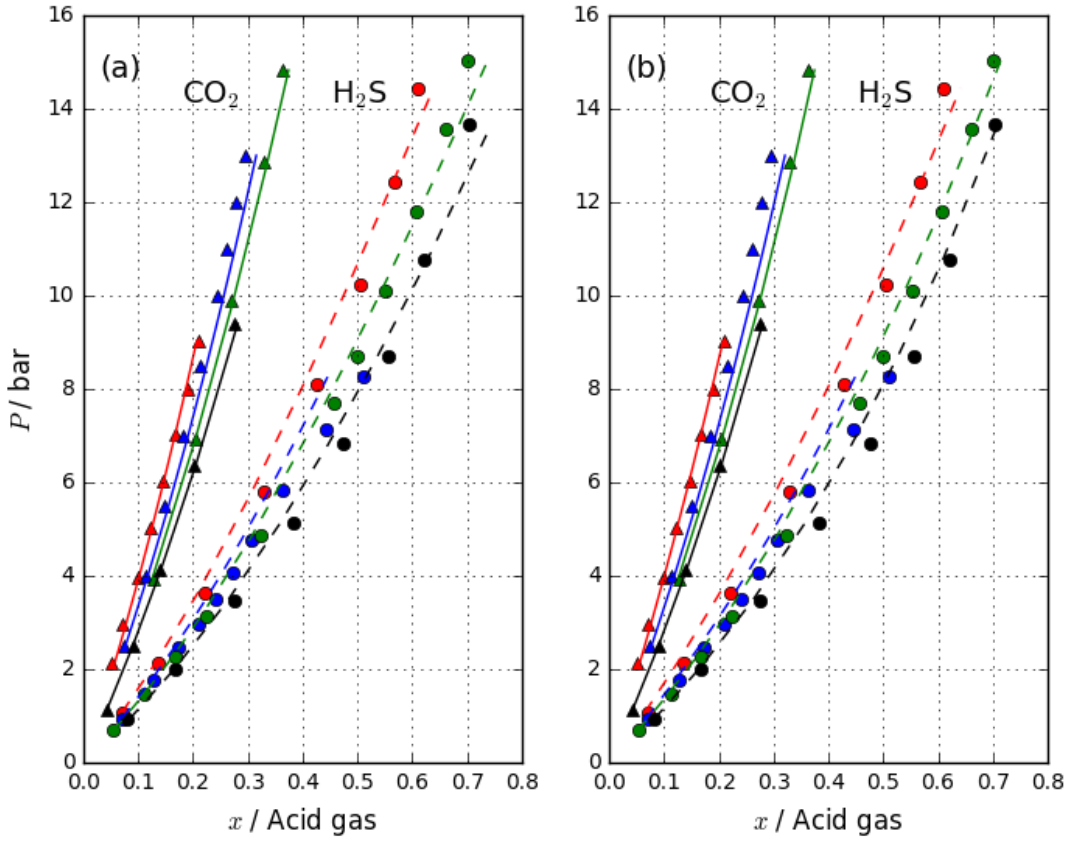

Figure 7: Solubility of acid gases in the studied ILs: (i) [C_2mim][NTf_2] (red), CO_2 at 298.15 K (solid) and H_2S at 303.15 K (dashed) (ii) [C_4mim][NTf_2] (blue), CO_2 at 298.15 K (solid) and H_2S at 303.15 K (dashed), (iii) [C_6mim][NTf_2] (green), CO_2 at 297.30 K (solid) and H_2S at 303.15 K (dashed) and (iv) [C_8mim][NTf_2] (black), CO_2 at 303.15 K (solid) and H_2S at 303.15 K (dashed). Symbols represent experimental data. Lines represent the predictions of PC-SAFT with the 4-site association scheme for (a) strategy 1 and (b) strategy 2 for CO_2 (solid) and H_2S (dashed).

Table 4: Solubility AARD for systems investigated in this study with the 4(2:2) association scheme and both strategies.

System	T K	P bar	Strategy 1 AARD %	Strategy 2 AARD %	Ref.
CO_2–[C_2mim][NTf_2]	298.15 – 450.5	2.00 – 337.29	7.20	5.00	[73], [74]
H_2S–[C_2mim][NTf_2]	303.15	1.08 – 14.44	3.73	5.66	[75]
CO_2–[C_4mim][NTf_2]	298.15	2.50 – 13.00	4.98	6.51	[76]
	333.3	18.12 – 130.19	9.80	6.70	[9]
H_2S–[C_4mim][NTf_2]	303.15	0.94 – 8.26	6.62	7.48	[77]
CO_2–[C_6mim][NTf_2]	297.30	3.94 – 14.83	1.54	1.82	[78]
H_2S–[C_6mim][NTf_2]	303.15	0.68 – 15.04	2.76	3.13	[6]
CO_2–[C_8mim][NTf_2]	303.15	1.12 – 9.40	1.77	1.45	[6]
	345	16.00 – 231.00	7.80	6.65	[79]
H_2S–[C_8mim][NTf_2]	303.15 – 323.15	0.93 – 17.39	5.05	14.56	[6]
CO_2–H_2S–[C_8mim][NTf_2]	303.15	1.72 – 9.60	H_2S: 6.24 CO_2: 7.99	H_2S:11.63 CO_2:9.10	[6]
	323.15	2.04 – 10.90	H_2S: 12.57 CO_2: 2.56	H_2S: 31.69 CO_2: 20.59	[6]
	343.15	2.24 – 12.08	H_2S: 15.37 CO_2: 6.67	H_2S: 34.69 CO_2: 25.48	[6]

nary interaction parameters to improve the solubility fit, high values of AARD for CO_2-IL system were reported (5.845%–14.825%).

The second strategy treats the IL as two charged ions: a cation and an anion; therefore, the electrolyte contribution is also taken into consideration in this strategy. The same model was used by Ji et al. [64], referred to as strategy 6 in their work; however, they did not account for the association in this strategy and did not consider H_2S solubility in their study. Ji et al. studied H_2S solubility in Ref. 81 and only by introducing binary interaction parameters was the e-PC-SAFT able to reliably describe the H_2S solubility. The results of both strategies are plotted and compared to the experimental solubility data reported in literature (see Figures 8 and 9).

The solubility of CO_2 in [C_2mim][NTf_2] and [C_8mim][NTf_2] at high pressure is also represented using the same set of parameters given in Table 2 and Table 3 for the 4-site scheme and for both strategies. The experimental data was reproduced with reasonable accuracy. No additional binary interaction parameters are needed. The results are shown in Figures 10, 11 and 12 and are detailed later.

PC-SAFT provides a better fit to the solubility of acid gases in ILs at low pressures than at high pressures. For the non-associating scheme, PC-SAFT overestimates the solubility at high pressures. This might be attributed to the fact that the association contribution becomes more important at high pressure. Moreover, H_2S is about twice more soluble in the ILs than CO_2. The solubility of both acid gases in [C_8mim][NTf_2] is higher than that in [C_6mim][NTf_2] than in [C_4mim][NTf_2] than in [C_2mim][NTf_2], which is in agreement with conclusions obtained in previous studies [9, 6]; the solubility of the acid gases in the IL increases with increasing alkyl chain length of the methylimidazolium cation.

The solubility fit improves by accounting for the association contribution which can be noticed in Figures 8 and 9. In most cases, the 4-sites association scheme provides the most accurate predictions for the solubility of both acid gases in the studied ILs without the need for any binary interaction parameters for fitting with an AARD of 2.76%–6.62% for H_2S-ILs systems and 1.54%–4.98% for CO_2-IL systems. By adding association sites, the segment diameter σ_i of the IL decreases and the number of segments decreases accordingly to keep the density of the IL fixed (see Tables 2 and 3). Consequently, the density of the IL increases leaving no space for the acid gas to penetrate into the IL causing the solubility of the acid gas to decrease. This can be seen in Figures 8 and 9. For this reason accounting for the association helped to improve the over estimated solubility of the non-associating scheme.

In strategy 2, the difference between different association schemes is found to be smaller compared to that of strategy 1 which can be noticed by comparing Figures 8 and 9. This indicates that the electrolyte term plays a similar role to the association term in improving the sol-

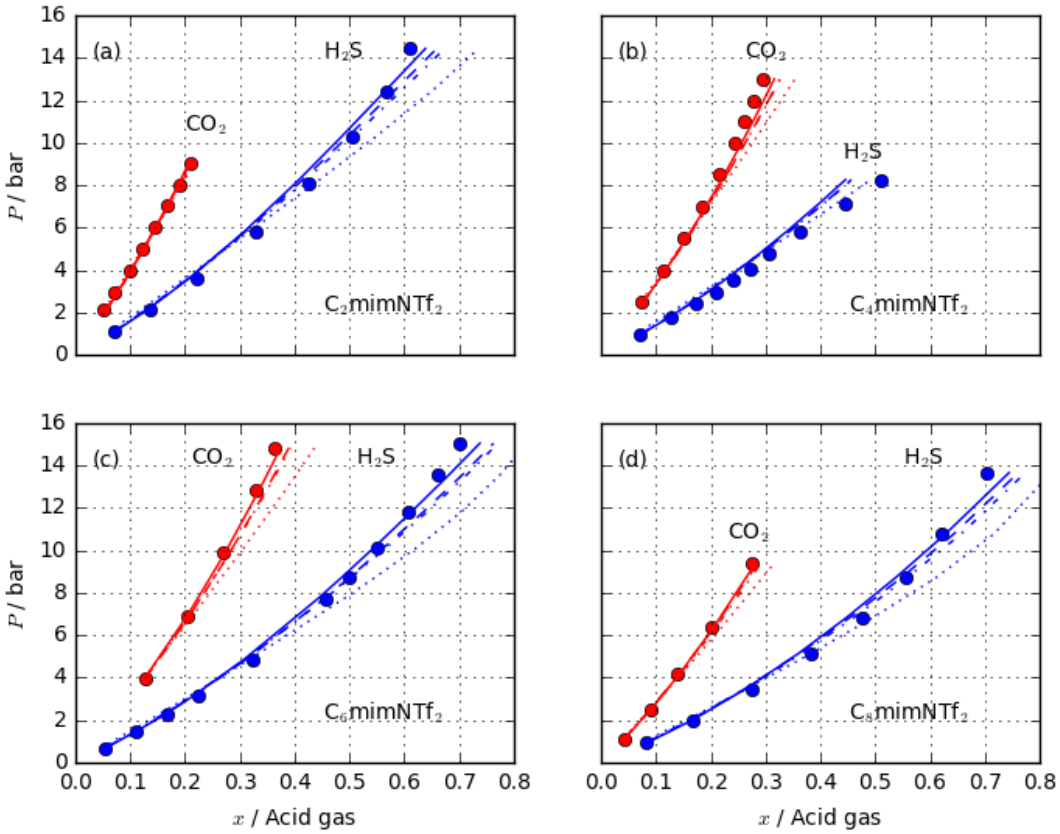

Figure 8: Binary solubility of CO_2 (red) and H_2S (blue) in the ILs (a) C_2mimNTf$_2$, CO_2 at 298.15 K and H_2S at 303.15 K, (b) C_4mimNTf$_2$, CO_2 at 298.15 K and H_2S at 303.15 K, (c) C_6mimNTf$_2$, CO_2 at 297.30 K and H_2S at 303.15 K and (d) C_8mimNTf$_2$, CO_2 at 303.15 K and H_2S at 303.15 K. The symbols represent experimental data. The lines represent the calculated solubilities using PC-SAFT with the ILs modelled in strategy 1 with (i) no association (dotted lines), (ii) 2-site association scheme (dashed-dotted lines), (iii) 3-site association scheme (dashed lines), and (iv) 4-site association scheme (solid lines).

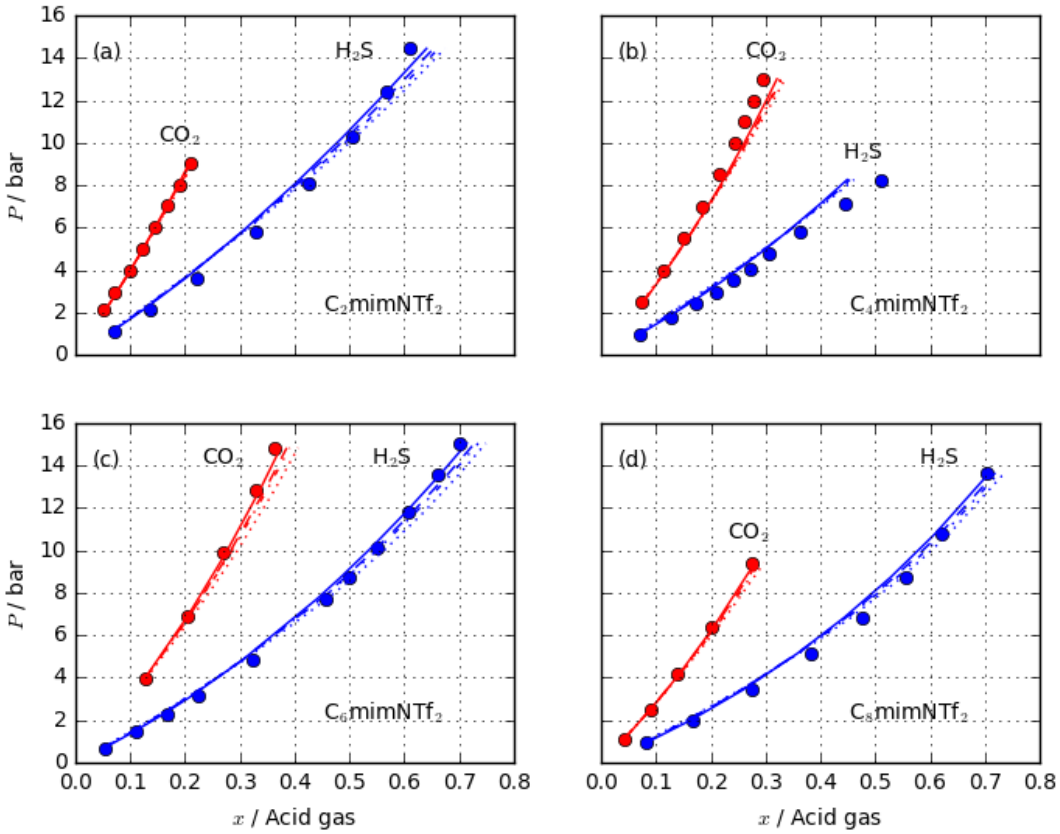

Figure 9: Binary solubility of CO_2 (red) and H_2S (blue) in the ILs (a) C_2mimNTf$_2$, CO_2 at 298.15 K and H_2S at 303.15 K, (b) C_4mimNTf$_2$, CO_2 at 298.15 K and H_2S at 303.15 K, (c) C_6mimNTf$_2$, CO_2 at 297.30 K and H_2S at 303.15 K and (d) C_8mimNTf$_2$, CO_2 at 303.15 K and H_2S at 303.15 K. The symbols represent experimental data. The lines represent the calculated solubilities using PC-SAFT with the ILs modelled in strategy 2 with (i) no association (dotted lines), (ii) 2-site association scheme (dashed-dotted lines), (iii) 3-site association scheme (dashed lines) (iv) 4-site association scheme (solid lines).

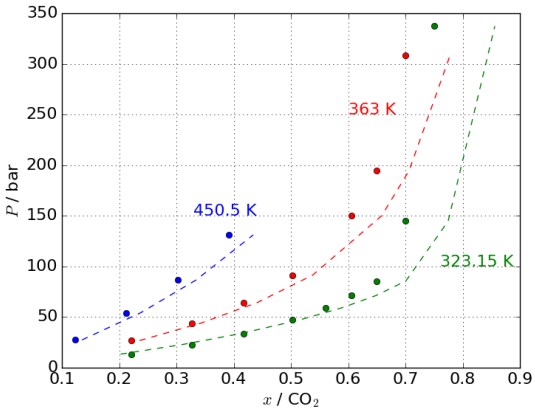

Figure 10: Solubility of CO_2 in [C_2mim][NTf_2] at different temperatures and high pressures. The symbols represent experimental data [73] and [74]. The lines are the calculations of PC-SAFT using strategy 1 with the 4-site association scheme.

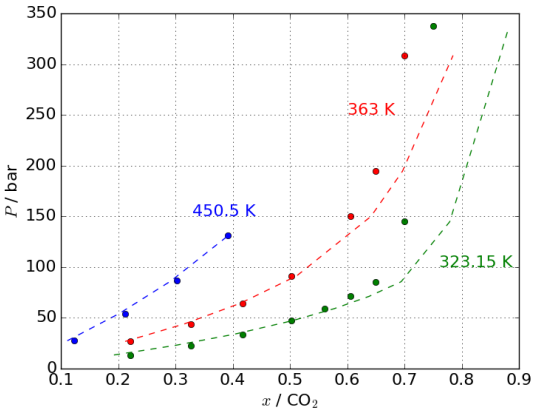

Figure 11: Solubility of CO_2 in [C_2mim][NTf_2] at different temperatures and high pressures: The symbols represent experimental data [73] and [74]. The lines are the calculations of PC-SAFT using strategy 2 with the 4-site association scheme.

ubility fit. At low pressures no significant improvement has been achieved by treating the IL as electrolytes in strategy 2. However, at high pressures the both the density and solubility fits are improved when strategy 2 is used. The model predictive capability is also enhanced by allowing to examine different ILs anion-cation combinations.

The solubility of CO_2 in ILs at high pressure is calculated using the same set of parameters without any additional binary parameters for both strategies. The experimental data are reproduced with reasonable accuracy. The results of CO_2 solubility in [C_2mim][NTf_2] for both strategies are shown in Figures 10 and 11 and Table 4. In the temperature range 298.15–450.5 K and pressure range 2–337.29 bar, strategy 2 (AARD 5.0%) provides a better description than strategy 1 (AARD 7.2%) of the measured CO_2 solubility in [C_2mim][NTf_2].

The high pressure solubility of CO_2 in [C_8mim][NTf_2] at 345 K is represented using both strategies. It can be noticed from Figure 12 that the low pressure solubility is more accurately represented using strategy 1, while strategy 2 slightly underestimates it. However, at pressures above 50 bar the solubility is more accurately represented using strategy 2.

The solubility of H_2S in [C_8mim][NTf_2] is also represented using the same set of parameters given in Table 2 for the 4-site scheme using strategy 1 at different temperatures. The experimental data from Jalili et al. [6] were reproduced with reasonable accuracy with AARD of 3.74% at 303.15 K, 5.1% at 313.5 K and 6.3% at 323.15 K (see Figure 13). No additional binary inter-

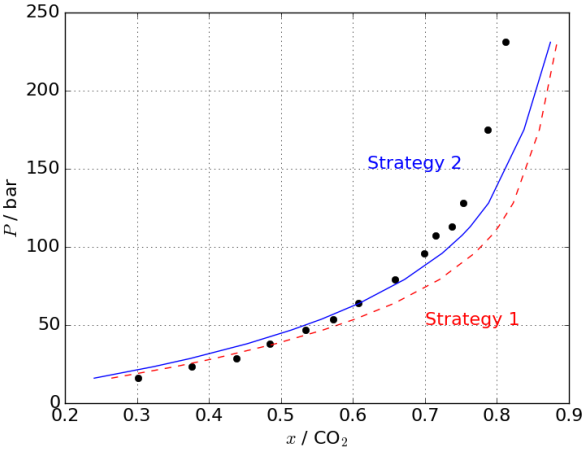

Figure 12: Solubility of CO_2 in [C_8mim][NTf_2] at 345 K and high pressures with the 4-site association scheme: The symbols represent experimental data [79].The dashed red line represents the calculations of PC-SAFT using strategy 1 and the solid blue line represents strategy 2.

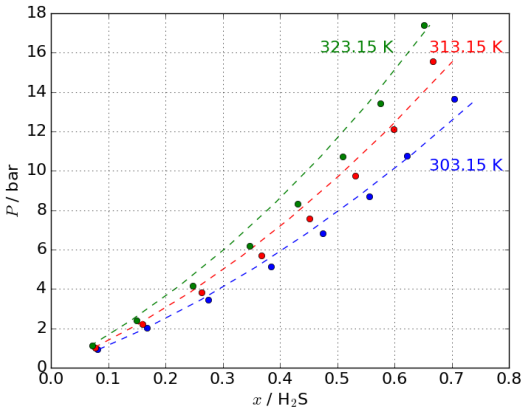

Figure 13: Solubility of H_2S in [C_8mim][NTf_2] at different temperatures: (i) 303.15 K (blue), (ii) 313.15 K (red) and (iii) 323.15 K (green). The symbols represent experimental data [6]. The dashed lines are the calculations of PC-SAFT using strategy 1 with the 4-site association scheme.

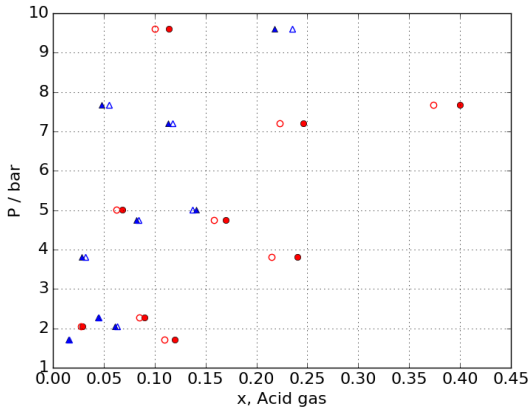

Figure 14: Ternary mixtures of CO_2-H_2S-C_8mimNTf_2 at 303.15 K with the 4-site association scheme (strategy 1). Open triangles represent the predicted CO_2 solubility using PC-SAFT, open circles represent the predicted H_2S solubility, and filled symbols represent experimental data [6].

action parameters were used. At this range of low pressures (0.935 bar – 17.395 bar), strategy 1 results in a significantly more accurate representation (AARD 5.0%) of this system than strategy 2 (AARD 14.59%). This leads to conclusion that the molecule-based strategy 1 is preferable at low pressures in representing the solubility of acid gases in ILs, while at high pressure the ion-based strategy 2 is preferable.

5. Ternary mixture CO_2-H_2S-C_8mimNTf_2

The optimum parameters obtained from the experimental density and binary solubility fit for the 4-sites association scheme of strategy 1 are also used to predict the solubility of the ternary system CO_2-H_2S-C_8mimNTf_2 at three different temperatures. The results are shown in Figures 14, 15, and 16. The experimental data from Ref. 6 are reproduced with an AARD of 6.24% for CO_2 and 7.99% for H_2S at 303.15 K, 2.59% for CO_2 and 12.57% for H_2S at 323.15 K and 6.67% for CO_2 and 15.37 % for H_2S at 343.15 K without the need for binary interaction parameters. Strategy 1 with the 4-site scheme parameters provided the best results for the ternary system. For example, the AARD of strategy 2 was found to be 9.1% for CO_2 and 11.63% for H_2S for the 4-site scheme at 303.15 K. Furthermore, the associating schemes provides better results than the non-associating schemes for both strategies. For instance, the AARD of the non-associating scheme of strategy 1 was found to be 14.6% for CO_2 and 8.90% for H_2S at 303.15 K. This was also the case for strategy 2 (see Table 4). For the ternary system, only low pressure data were available (1.72–12.08 bar) and at this range of pressures, strategy 1 provided significantly better results than strategy 2. This is consistent with the binary system results obtained in Section 4.

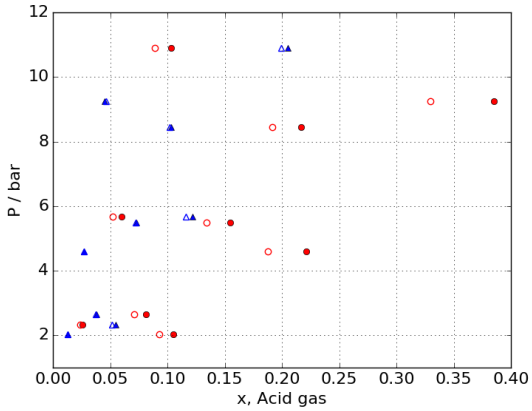

Figure 15: Ternary mixtures of CO_2-H_2S-C_8mimNTf_2 at 323.15 K with the 4-site association scheme (strategy 1). Open triangles represent the predicted CO_2 solubility using PC-SAFT, open circles represent the predicted H_2S solubility, and filled symbols represent experimental data [6].

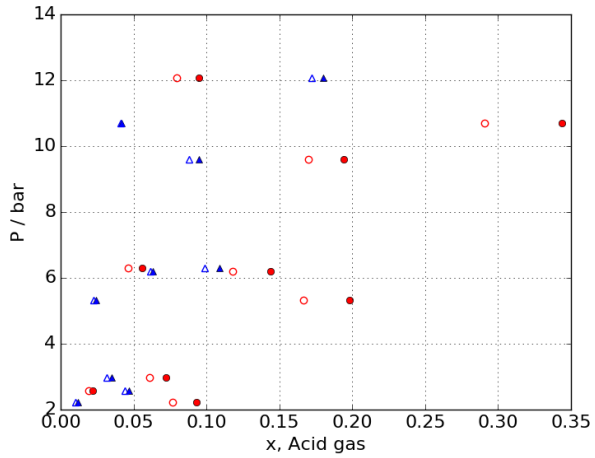

Figure 16: Ternary mixtures of CO_2-H_2S-C_8mimNTf$_2$ at 343.15 K with the 4-site association scheme (strategy 1). Open triangles represent the predicted CO_2 solubility using PC-SAFT, open circles represent the predicted H_2S solubility, and filled symbols represent experimental data [6].

6. Conclusion

ILs have the potential to significantly improve the safety, economics, and environmental sustainability of acid gas removal processes. In this work, we explored the use of PC-SAFT to quantitatively describe the thermodynamics of acid-gases in several methylimidazolium bis (trifluoromethylsulfonyl) imide ionic liquids. Firstly, we examined the use of treating the IL as either a system of neutral molecules or as separate cations and anions, where an electrolyte term is added to the free energy model. The inclusion of the electrolyte term improves the high pressure density and solubility fit, whereas its effect is insignificant at low pressures. The predictive capability is enhanced by allowing the description of different ILs anion-cation combinations without the need for additional experimental data.

In addition, we examined the effect of using different self-association schemes for the ILs. By selecting the proper association scheme, the solubility of acid gases in ILs can be accurately described using PC-SAFT with AARD ranging from 1.54% to 6.62%. This yields a significant improvement to the accuracy of PC-SAFT for these systems without the need to include empirical binary interaction parameters, as was required in previous studies.

Acknowledgments

HA greatfully acknowledges financial support from the Libyan Ministry of Higher Education and Scientific Research.

References

[1] D. Huo, The Global Sour Gas Problem, Tech. rep., Stanford University (November 2012).

[2] B. Shimekit, H. Mukhtar, Natural Gas Purification Technologies - Major Advances for CO_2 Separation and Future Directions, Advances in Natural Gas Technology, InTech, 2012. doi:10.5772/2324.

[3] S. Kumar, J. Cho, I. Moon, Ionic liquid-amine blends and CO_2 BOLs: Prospective solvents for natural gas sweetening and CO_2 capture technology: A review, Int. J. Greenhouse Gas Control 20 (0) (2014) 87 – 116. doi:10.1016/j.ijggc.2013.10.019.

[4] F. Karadas, M. Atilhan, S. Aparicio, Review on the Use of Ionic Liquids (ILs) as Alternative Fluids for CO_2 Capture and Natural Gas Sweetening, Energy Fuels 24 (11) (2010) 5817–5828. doi:10.1021/ef1011337.

[5] T. Welton, Ionic liquids in catalysis, Coord. Chem. Rev. 248 (21-24) (2004) 2459–2477. doi:10.1016/j.ccr.2004.04.015.

[6] A. H. Jalili, M. Safavi, C. Ghotbi, A. Mehdizadeh, M. Hosseini-Jenab, V. Taghikhani, Solubility of CO_2, H_2S, and Their Mixture in the Ionic Liquid 1-Octyl-3-methylimidazolium Bis(trifluoromethyl)sulfonylimide, J. Phys. Chem. B 116 (9) (2012) 2758–2774. doi:10.1021/jp2075572.

[7] M. Freemantle, An Introduction to Ionic Liquids, The Royal Society of Chemistry, 2010, ISBN 978-1-84755-161-0.

[8] A. Kamps, D. Tuma, J. Xia, G. Maurer, Solubility of CO_2 in the ionic liquid [bmim][PF_6], J. Chem. Eng. Data 48 (3) (2003) 746–749. doi:10.1021/je034023f.

[9] S. N. V. K. Aki, B. R. Mellein, E. M. Saurer, J. F. Brennecke, High-Pressure Phase Behavior of Carbon Dioxide with Imidazolium-Based Ionic Liquids, J. Phys. Chem. B 108 (52) (2004) 20355–20365. doi:10.1021/jp046895+.

[10] A. Shariati, K. Gutkowski, C. J. Peters, Comparison of the phase behavior of some selected binary systems with ionic liquids, AIChE J. 51 (5) (2005) 1532–1540. doi:10.1002/aic.10384.

[11] E. D. Bates, R. D. Mayton, I. Ntai, J. H. Davis, CO_2 Capture by a Task-Specific Ionic Liquid, J. Am. Chem. Soc. 124 (6) (2002) 926–927. doi:10.1021/ja017593d.

[12] L. G. Sanchez, G. Meindersma, A. de Haan, Solvent Properties of Functionalized Ionic Liquids for CO_2 Absorption, Chem. Eng. Res. Des. 85 (1) (2007) 31 – 39. doi:10.1205/cherd06124.

[13] D. Camper, J. E. Bara, D. L. Gin, R. D. Noble, Room-Temperature Ionic Liquid-Amine Solutions: Tunable Solvents for Efficient and Reversible Capture of CO_2, Ind. Eng. Chem. Res. 47 (21) (2008) 8496–8498. doi:10.1021/ie801002m.

[14] F.-Y. Jou, A. Mather, Solubility of Hydrogen Sulfide in [bmim][PF_6], Int. J. Thermophys. 28 (2) (2007) 490–495. doi:10.1007/s10765-007-0185-z.

[15] C. S. Pomelli, C. Chiappe, A. Vidis, G. Laurenczy, P. J. Dyson, Influence of the interaction between hydrogen sulfide and ionic liquids on solubility: experimental and theoretical investigation, J. Phys. Chem. B 111 (45) (2007) 13014–13019. doi:10.1021/jp076129d.

[16] Y. J. Heintz, L. Sehabiague, B. I. Morsi, K. L. Jones, D. R. Luebke, H. W. Pennline, Hydrogen Sulfide and Carbon Dioxide Removal from Dry Fuel Gas Streams Using an Ionic Liquid as a Physical Solvent, Energy Fuels 23 (10) (2009) 4822–4830. doi:10.1021/ef900281v.

[17] A. H. Jalili, A. Mehdizadeh, M. Shokouhi, A. N. Ahmadi, M. Hosseini-Jenab, F. Fateminassab, Solubility and diffusion of CO_2 and H_2S in the ionic liquid 1-ethyl-3-methylimidazolium ethylsulfate, J. Chem. Thermodyn. 42 (10) (2010) 1298 – 1303. doi:10.1016/j.jct.2010.05.008.

[18] E. Hawlicka, T. Dlugoborski, Molecular dynamics simulations of the aqueous solution of tetramethylammonium chloride, Chem. Phys. Lett. 268 (56) (1997) 325 – 330. doi:10.1016/S0009-2614(97)00229-7.

[19] J. Oberbrodhage, Phase transfer catalysts between polar and non-polar media: a molecular dynamics simulation of tetrabutylammonium iodide at the formamide-hexane interface, Phys. Chem. Chem. Phys. 2 (2000) 129–135. doi:10.1039/A907612C.

[20] C. G. Hanke, N. A. Atamas, R. M. Lynden-Bell, Solvation of small molecules in imidazolium ionic liquids: a simulation study, Green Chem. 4 (2002) 107–111. doi:10.1039/B109179B.

[21] T. I. Morrow, , E. J. Maginn, Molecular Dynamics Study of the Ionic Liquid 1-n-Butyl-3-methylimidazolium Hexafluorophosphate, J. Phys. Chem. B 106 (49) (2002) 12807–12813. doi:10.1021/jp0267003.

[22] X. Liu, S. Zhang, G. Zhou, G. Wu, X. Yuan, X. Yao, New Force Field for Molecular Simulation of Guanidinium-Based Ionic Liquids, J. Phys. Chem. B 110 (24) (2006) 12062–12071. doi:10.1021/jp060834p.

[23] S. Tsuzuki, W. Shinoda, H. Saito, M. Mikami, H. Tokuda, M. Watanabe, Molecular Dynamics Simulations of Ionic Liquids: Cation and Anion Dependence of Self-Diffusion Coefficients of Ions, J. Phys. Chem. B 113 (31) (2009) 10641–10649. doi:10.1021/jp811128b.

[24] S. Feng, G. A. Voth, Molecular dynamics simulations of imidazolium-based ionic liquid/water mixtures: Alkyl side chain length and anion effects, Fluid Phase Equilib. 294 (12) (2010) 148 – 156. doi:10.1016/j.fluid.2010.02.034.

[25] G. Hantal, I. Voroshylova, M. N. D. S. Cordeiro, M. Jorge, A systematic molecular simulation study of ionic liquid surfaces using intrinsic analysis methods, Phys. Chem. Chem. Phys. 14 (2012) 5200–5213. doi:10.1039/C2CP23967A.

[26] B. Yoo, J. K. Shah, Y. Zhu, E. J. Maginn, Amphiphilic interactions of ionic liquids with lipid biomembranes: a molecular simulation study, Soft Matter 10 (2014) 8641–8651. doi:10.1039/C4SM01528B.

[27] L. F. Vega, O. Vilaseca, F. Llovell, J. S. Andreu, Modeling ionic liquids and the solubility of gases in them: Recent advances and perspectives, Fluid Phase Equilib. 294 (12) (2010) 15 – 30. doi:10.1016/j.fluid.2010.02.006.

[28] A. Shariati, C. J. Peters, High pressure phase behavior of systems with ionic liquids: measurements and modeling of the binary system fluoroform+1-ethyl-3-methylimidazolium hexafluorophosphate, J. Supercrit. Fluids 25 (2) (2003) 109 – 117. doi:10.1016/S0896-8446(02)00160-2.

[29] M. B. Shiflett, A. Yokozeki, Solubilities and Diffusivities of Carbon Dioxide in Ionic Liquids: [bmim][PF_6] and [bmim][BF_4], Ind. Eng. Chem. Res. 44 (12) (2005) 4453–4464. doi:10.1021/ie058003d.

[30] D. Y. Peng, D. B. Robinson, A new two-constant equation of state, Ind. Eng. Chem. Fund 15 (1) (1976) 59–64. doi:10.1021/i160057a011.

[31] S. Giorgio, Equilibrium constants from a modified Redlich-Kwong equation of state, Chem. Eng. Sci. 27 (6) (1972) 1197 – 1203. doi:10.1016/0009-2509(72)80096-4.

[32] H. Renon, J. M. Prausnitz, Local compositions in thermodynamic excess functions for liquid mixtures, AIChE J. 14 (1) (1968) 135–144. doi:10.1002/aic.690140124.

[33] D. S. Abrams, J. M. Prausnitz, Statistical thermodynamics of liquid mixtures: A new expression for the excess gibbs energy of partly or completely miscible systems., AIChE J. 21 (1) (1975) 116–128.

[34] U. Domanska, A. Marciniak, Phase behaviour of 1-hexyloxymethyl-3-methyl-imidazolium and 1,3-dihexyloxymethyl-imidazolium based ionic liquids with alcohols, water, ketones and hydrocarbons: The effect of cation and anion on solubility, Fluid Phase Equilib. 260 (1) (2007) 9 – 18. doi:10.1016/j.fluid.2006.07.005.

[35] T. Banerjee, M. K. Singh, R. K. Sahoo, A. Khanna, Volume, surface and {UNIQUAC} interaction parameters for imidazolium based ionic liquids via Polarizable Continuum Model, Fluid Phase Equilib. 234 (12) (2005) 64 – 76. doi:10.1016/j.fluid.2005.05.017.

[36] A. Fredenslund, R. L. Jones, J. M. Prausnitz, Group-contribution estimation of activity coefficients in nonideal liquid mixtures, AIChE J. 21 (6) (1975) 1086–1099. doi:10.1002/aic.690210607.

[37] U. Weidlich, J. Gmehling, A modified UNIFAC model. 1. Prediction of VLE, h^E and γ^∞, Ind. Eng. Chem. Res. 26 (7) (1987) 1372–1381. doi:10.1021/ie00067a018.

[38] Y. Gaston-Bonhomme, P. Petrino, J. Chevalier, UNIFACVISCO group contribution method for predicting kinematic viscosity: extension and temperature dependence, Chem. Eng. Sci. 49 (11) (1994) 1799 – 1806. doi:10.1016/0009-2509(94)80065-0.

[39] N. Zhao, R. Oozeerally, V. Degirmenci, Z. Wagner, M. Bendová, J. Jacquemin, New Method Based on the UNIFACVISCO Model for the Estimation of Ionic Liquids Viscosity Using the Experimental Data Recommended by Mathematical Gnostics, J. Chem Eng Data 61 (11) (2016) 3908–3921. arXiv:http://dx.doi.org/10.1021/acs.jced.6b00689, doi:10.1021/acs.jced.6b00689.
URL `http://dx.doi.org/10.1021/acs.jced.6b00689`

[40] N. Zhao, J. Jacquemin, R. Oozeerally, V. Degirmenci, New Method for the Estimation of Viscosity of Pure and Mixtures of Ionic Liquids Based on the UNIFACVISCO Model, J. Chem. Eng. Data 61 (6) (2016) 2160–2169. arXiv:http://dx.doi.org/10.1021/acs.jced.6b00161, doi:10.1021/acs.jced.6b00161.

[41] R. Kato, J. Gmehling, Systems with ionic liquids: Measurement of VLE and γ^∞ data and prediction of their thermodynamic behavior using original UNIFAC, mod. UNIFAC(Do) and COSMO-RS(Ol), J. Chem. Thermodyn. 37 (6) (2005) 603 – 619. doi:10.1016/j.jct.2005.04.010.

[42] E. I. Alevizou, G. D. Pappa, E. C. Voutsas, Prediction of phase equilibrium in mixtures containing ionic liquids using UNIFAC, Fluid Phase Equilib. 284 (2) (2009) 99 – 105. doi:10.1016/j.fluid.2009.06.012.

[43] S. Nebig, R. Bolts, J. Gmehling, Measurement of vapor liquid equilibria (vle) and excess enthalpies (he) of binary systems with 1-alkyl-3-methylimidazolium bis(trifluoromethylsulfonyl)imide and prediction of these properties and γ^∞ using modified UNIFAC (dortmund), Fluid Phase Equilib. 258 (2) (2007) 168 – 178. doi:10.1016/j.fluid.2007.06.001.

[44] A. Klamt, Conductor-like Screening Model for Real Solvents: A New Approach to the Quantitative Calculation of Solvation Phenomena, J. Phys. Chem. 99 (7) (1995) 2224–2235. doi:10.1021/j100007a062.

[45] U. Domanska, A. Pobudkowska, F. Eckert, (Liquid + liquid) phase equilibria of 1-alkyl-3-methylimidazolium methylsulfate with alcohols, or ethers, or ketones, J. Chem. Thermodyn. 38 (6) (2006) 685–695. doi:10.1016/j.jct.2005.07.024.

[46] T. Banerjee, M. Singh, A. Khanna, Prediction of binary VLE of imidazolium-based ionic liquids by COSMU-RS, Ind. Eng. Chem. Res. 45 (20) (2006) 6876. doi:10.1021/ie061107j.

[47] M. Freire, L. Santos, I. Marrucho, J. Coutinho, Evaluation of COSMO-RS for the prediction of LLE and VLE of alcohols + ionic liquids, Fluid Phase Equilib. 255 (2) (2007) 167–178. doi:10.1016/j.fluid.2007.04.020.

[48] W. G. Chapman, K. E. Gubbins, G. Jackson, M. Radosz, New reference equation of state for associating liquids, Ind. Eng. Chem. Res. 29 (8) (1990) 1709–1721. doi:10.1021/ie00104a021.

[49] S. H. Huang, M. Radosz, Equation of state for small, large, polydisperse, and associating molecules, Ind. Eng. Chem. Res. 29 (11) (1990) 2284–2294. doi:10.1021/ie00107a014.

[50] A. Gil-Villegas, A. Galindo, P. J. Whitehead, S. J. Mills, G. Jackson, A. N. Burgess, Statistical associating fluid theory for chain molecules with attractive potentials of variable range, J. Chem. Phys 106 (10) (1997) 4168–4186. doi:10.1063/1.473101.

[51] F. J. Blas, L. F. Vega, Thermodynamic behaviour of homonuclear and heteronuclear Lennard-Jones chains with association sites from simulation and theory, Mol. Phys. 92 (1) (1997) 135–150. doi:10.1080/002689797170707.

[52] A. Lymperiadis, C. S. Adjiman, A. Galindo, G. Jackson, A group contribution method for associating chain molecules based on the statistical associating fluid theory (SAFT-γ), J. Phys. Chem. 127 (23) (2007) 234903. doi:10.1063/1.2813894.

[53] E. K. Karakatsani, I. G. Economou, Perturbed Chain-Statistical Associating Fluid Theory Extended to Dipolar and Quadrupolar Molecular Fluids, J. Phys. Chem. B 110 (18) (2006) 9252–9261. doi:10.1021/jp056957b.

[54] M. Rahmati-Rostami, B. Behzadi, C. Ghotbi, Thermodynamic modeling of hydrogen sulfide solubility in ionic liquids using modified SAFT-VR and PC-SAFT equations of state, Fluid Phase Equilib. 309 (2) (2011) 179 – 189. doi:10.1016/j.fluid.2011.07.013.

[55] M. C. Kroon, E. K. Karakatsani, I. G. Economou, G. J. Witkamp, C. J. Peters, Modeling of the Carbon Dioxide Solubility in Imidazolium-Based Ionic Liquids with the tPC-PSAFT Equation of State, J. Phys. Chem. B 110 (18) (2006) 9262–9269. doi:10.1021/jp060300o.

[56] F. Llovell, E. Valente, O. Vilaseca, L. F. Vega, Modeling Complex Associating Mixtures with [$C_n$mim][Tf_2N] Ionic Liquids: Predictions from the Soft-SAFT Equation, J. Phys. Chem. B 115 (15) (2011) 4387–4398. doi:10.1021/jp112315b.

[57] S. Ashrafmansouri, S. Raeissi, Modeling gas solubility in ionic liquids with the SAFT-γ group contribution method, J. Supercrit. Fluids 63 (2012) 81 – 91. doi:10.1016/j.supflu.2011.12.014.

[58] J. Gross, G. Sadowski, Perturbed Chain SAFT: An Equation of State Based on a Perturbation Theory for Chain Molecules, Ind. Eng. Chem. Res. 40 (4) (2001) 1244–1260. doi:10.1021/ie0003887.

[59] P. A. Hunt, C. R. Ashworth, R. P. Matthews, Hydrogen bonding in ionic liquids, Chem. Soc. Rev. 44 (2015) 1257–1288. doi:10.1039/C4CS00278D.

[60] B. D. Mather, Non-covalent interactions in block copolymers synthesized via living polymerization techniques, Ph.D. thesis, Virginia Polytechnic Institute and State University (2007).

[61] P. Debye, E. Hückel, On the theory of electrolytes i. freezing point depression and related phenomena, Phys. Z. 24 (9) (1923) 185–206.

[62] C. Held, L. F. Cameretti, G. Sadowski, Modeling aqueous electrolyte solutions: Part 1. Fully dissociated electrolytes, Fluid Phase Equilib. 270 (12) (2008) 87 – 96. doi:10.1016/j.fluid.2008.06.010.

[63] L. F. Cameretti, G. Sadowski, J. M. Mollerup, Modeling of Aqueous Electrolyte Solutions with Perturbed-Chain Statistical Associated Fluid Theory, Ind. Eng. Chem. Res. 44 (9) (2005) 3355–3362. doi:10.1021/ie0488142.

[64] X. Ji, C. Held, G. Sadowski, Modeling imidazolium-based ionic liquids with ePC-SAFT, Fluid Phase Equilib. 335 (2012) 64 – 73. doi:10.1016/j.fluid.2012.05.029.

[65] K. Nasrifar, A. Tafazzol, Vapor Liquid Equilibria of Acid Gas Aqueous Ethanolamine Solutions Using the PCSAFT Equation of State, Ind. Eng. Chem. Res. 49 (16) (2010) 7620–7630. doi:10.1021/ie901181n.

[66] E.W. Lemmon and M.O. McLinden and D.G. Friend, "Thermophysical Properties of Fluid Systems" in **NIST Chemistry WebBook, NIST Standard Reference Database Number 69**, Eds. P.J. Linstrom and W.G. Mallard, National Institute of Standards and Technology, Gaithersburg MD, 2089, retrieved October 6, 2016. doi:10.18434/T4D303.

[67] J. Jacquemin, P. Husson, V. Mayer, I. Cibulka, High-Pressure Volumetric Properties of Imidazolium-Based Ionic Liquids: Effect of the Anion, J. Chem. Eng. Data 52 (6) (2007) 2204–2211. doi:10.1021/je700224j.

[68] J. Kumelan, A. P. S. Kamps, D. Tuma, G. Maurer, Solubility of CO_2 in the ionic liquid [hmim][Tf_2N], J. Chem. Thermodyn. 38 (11) (2006) 1396 – 1401. doi:10.1016/j.jct.2006.01.013.

[69] D. Santos, M. Santos, E. Franceschi, C. Dariva, A. Barison, S. Mattedi, Experimental Density of Ionic Liquids and Thermodynamic Modeling with Group Contribution Equation of State Based on the Lattice Fluid Theory, J. Chem. Eng. Data 61 (1) (2015) 348353. doi:10.1021/acs.jced.5b00592.

[70] M. Newville, T. Stensitzki, D. B. Allen, A. Ingargiola, LMFIT: Non-linear least-square minimization and curve-fitting for Python (2014). doi:10.5281/zenodo.11813.

[71] J. Safarov, W. A. El-Awady, A. Shahverdiyev, E. Hassel, Thermodynamic Properties of 1-Ethyl-3-methylimidazolium Bis(trifluoromethylsulfonyl)imide, J. Chem. Eng. Data 56 (1) (2011) 106–112. arXiv:http://dx.doi.org/10.1021/je100945u, doi:10.1021/je100945u.

[72] K. R. Harris, M. Kanakubo, L. A. Woolf, Temperature and Pressure Dependence of the Viscosity of the Ionic Liquids 1-Hexyl-3-methylimidazolium Hexafluorophosphate and 1-Butyl-3-methylimidazolium Bis(trifluoromethylsulfonyl)imide, J. Chem Eng Data 52 (3) (2007) 1080–1085. arXiv:http://dx.doi.org/10.1021/je700032n, doi:10.1021/je700032n.

[73] P. J. Carvalho, V. H. Alvarez, J. J. Machado, J. Pauly, J.-L. Daridon, I. M. Marrucho, M. Aznar, J. A. Coutinho, High pressure phase behavior of carbon dioxide in 1-alkyl-3-methylimidazolium bis(trifluoromethylsulfonyl)imide ionic liquids, J. Supercrit. Fluids 48 (2) (2009) 99 – 107. doi:10.1016/j.supflu.2008.10.012.

[74] A. M. Schilderman, S. Raeissi, C. J. Peters, Solubility of carbon dioxide in the ionic liquid 1-ethyl-3-methylimidazolium bis(trifluoromethylsulfonyl)imide, Fluid Phase Equilib. 260 (1) (2007) 19 – 22. doi:10.1016/j.fluid.2007.06.003.

[75] H. Sakhaeinia, A. H. Jalili, V. Taghikhani, A. A. Safekordi, Solubility of H_2S in Ionic Liquids 1-Ethyl-3-methylimidazolium Hexafluorophosphate ([emim][PF6]) and 1-Ethyl-3-methylimidazolium Bis(trifluoromethyl)sulfonylimide ([emim][Tf_2N]), J. Chem. Eng. Data 55 (12) (2010) 5839–5845. doi:10.1021/je100794k.

[76] J. L. Anthony, J. L. Anderson, E. J. Maginn, J. F. Brennecke, Anion Effects on Gas Solubility in Ionic Liquids, J. Phys. Chem. B 13 (109) (2005) 6366–6374. doi:DOI: 10.1021/jp046404l.

[77] A. H. Jalili, M. Rahmati-Rostami, C. Ghotbi, M. Hosseini-Jenab, A. N. Ahmadi, Solubility of H_2S in Ionic Liquids [bmim][PF_6], [bmim][BF_4], and [bmim][Tf_2N], J. Chem. Eng. Data 54 (6) (2009) 1844–1849. doi:10.1021/je8009495.

[78] M. B. Shiflett, A. Yokozeki, Solubility of CO_2 in Room Tem-

perature Ionic Liquid [hmim] [Tf_2N], J. Phys. Chem. B 111 (8) (2007) 2070–2074. doi:10.1021/jp067627.

[79] E.-K. Shin, B.-C. Lee, J. S. Lim, High-pressure solubilities of carbon dioxide in ionic liquids: 1-Alkyl-3-methylimidazolium bis(trifluoromethylsulfonyl)imide, J. Supercrit. Fluids 45 (3) (2008) 282 – 292. doi:10.1016/j.supflu.2008.01.020.

[80] Y. Chen, F. Mutelet, J. N. Jaubert, Modeling the Solubility of Carbon Dioxide in Imidazolium Based Ionic Liquids with the PCSAFT Equation of State, J. Phys. Chem. B 116 (49) (2012) 14375–14388. doi:10.1021/jp309944t.

[81] X. Ji, C. Held, G. Sadowski, Modeling imidazolium-based ionic liquids with ePC-SAFT. Part II. Application to H_2S and synthesis-gas components, Fluid Phase Equilib. 363 (2014) 59 – 65. doi:10.1016/j.fluid.2013.11.019.